PHYSOR 2004 -The Physics of Fuel Cycles and Advanced Nuclear Systems: Global Developments
Chicago, Illinois, April 25-29, 2004, on CD-ROM, American Nuclear Society, Lagrange Park, IL. (2004)

DYNAMICS OF A REDUCED ORDER NATURAL CIRCULATION BWR MODEL

Quan Zhou* and Rizwan-uddin
Department of Nuclear, Plasma and Radiological Engineering
University of Illinois, 103 S. Goodwin Ave.,Urbana, IL 61801 USA

Stability and bifurcation analyses of a new natural circulation BWR model that allows local pressure dependence of water saturation enthalpy and includes fundamental and first azimuthal modes for neutronics are presented. Stability boundaries (SBs) and 7.5% oscillation curves (representing natures of bifurcation along SBs) are plotted in inlet subcooling—external reactivity parameter space. Stability and bifurcation analyses show that both in-phase and out-of-phase oscillations as well as supercritical and subcritical bifurcations can occur along the SBs. Results of numerical simulations agree with those of stability and bifurcation analyses. Effects of several design and operating parameters on the stability of a natural circulation BWR are also reported.

KEYWORDS: Natural circulation, BWR, Stability, Bifurcation

1. Introduction

Natural circulation is a promising design feature for next generation of BWRs. Safety and economics of nuclear reactors can be improved through simplicity and passive features of the natural circulation design [1].

One of the primary concerns for safe operation of BWRs is stability. Both natural and forced circulation BWR systems, however, are susceptible to nuclear coupled density wave oscillations (DWOs) under certain adverse operating conditions [2]. DWOs can be either in-phase or out-of-phase type [3]. The former corresponds to global power and flow oscillations, and is excited by fundamental neutronic mode. The latter corresponds to regional oscillations (usually power of half of the core oscillates out-of-phase against the other half), and is an outcome of the first azimuthal mode. For natural circulation systems, experiments and analytical studies show other instability mechanisms besides DWOs. An important one of these is flashing-induced oscillation during start-up. Flashing, that is boiling in the unheated riser above the core, is caused due to local pressure drop. Flashing occurs most frequently under low system pressure during start-up. Jiang et al. [4] indicated that "the maximum void fraction caused by flashing is about 5% under a system pressure of 1.5 MPa, and about 80% under 0.1 MPa."

Several experimental studies of two-phase natural circulation system have been reported [5-7]. Although a few analytical studies [4, 8-9] have been carried out for natural circulation systems, they are limited in scope due to one or more of the following reasons:

- Many existing system codes are not designed to analyze natural circulation system. Those suitable to analyze the flashing phenomenon are too cumbersome for parametric studies.

* Corresponding author, Tel. 217-244-7600, FAX 217-333-2906, E-mail: quanzhou@uiuc.edu

- Existing reduced order models are too simplistic. Hence, some key features of system dynamics may be lost.
- There are limited reduced-order analyses of coupled models of thermal-hydraulics, fuel dynamics and neutronics.

Taking advantage of the two-mode neutronics and sophisticated fuel dynamics model, first developed by Karve et al [10], we present stability and bifurcation analyses of a two channel, nuclear-coupled, natural circulation BWR model. Two-phase thermal-hydraulics model is based on one we reported earlier. This model has been used to study the stability of two-phase natural circulation system (without neutronics) [11].

Reduced order model is presented in Section 2. A brief review of our approach for the stability and bifurcation analysis of the reduced order model is also given. Results of stability, bifurcation and numerical simulations are presented in Section 3, and the last section concludes the paper.

2. Reduced Order Model

2.1 Thermal-Hydraulic Model

The system considered in the model is shown in Figure 1. It is comprised of two heated channels (each of which represents a half of the core), two separate risers above the channels and a common down comer. A system pressure is imposed by setting the pressure at outlet of the risers, P_{exit}, to a fixed value. Some additional system parameters are also shown in Figure 1.

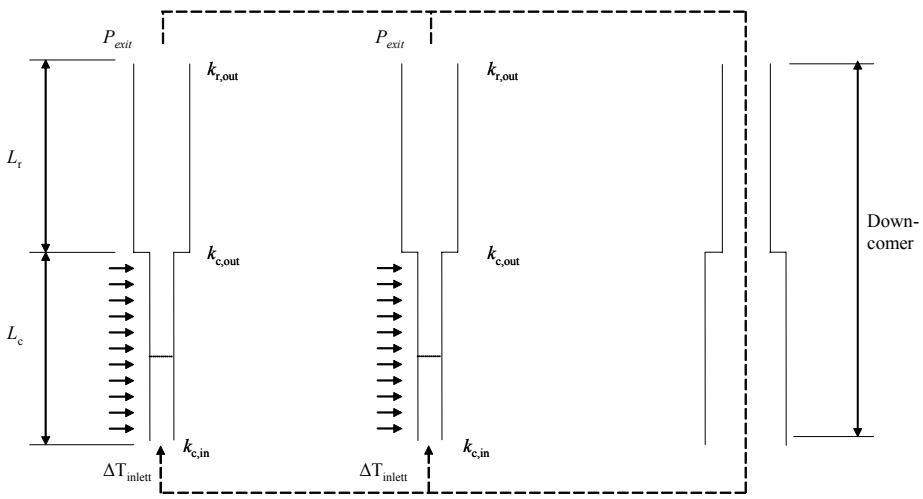

Fig. 1 Schematic plot of natural circulation system

The thermal-hydraulic model is based on the following two assumptions:

- Saturation enthalpy varies linearly with local pressure. Other thermal properties of water and steam are constant.
- Two phase flow can be modelled by Homogeneous Equilibrium Model (HEM)

Although better assumptions such as quadratic pressure dependence and non-equilibrium two-phase flow models can be applied, they will greatly increase complexity and decrease computational efficiency of the model.

Three cases, based on the location of the boiling boundary, are considered separately. These are shown in Figures 2a, 2b and 2c. For case 1, water enthalpy at the core exit is less than the saturation enthalpy, and flashing occurs in the riser. For case 2, because of relatively

large heat input, water starts boiling in the core. Case 3 is a degenerate case, in which water enthalpy is less than the saturation value at the core exit, but greater at the entrance of the riser due to local pressure loss.

Non-dimensional forms of continuity, energy and momentum partial differential equations are used to derive the dynamical system. Note that pressure dependence of water saturation enthalpy leads to modified forms of energy and momentum equations [12]. A weighted residual approach is employed to reduce the PDEs to a set of ODEs. Single phase and two-phase regions along the core and riser are discretized by arbitrary numbers of equal-sized nodes. In each node, spatially linear trial functions with time-dependent parameters for enthalpy (saturated or unsaturated), steam quality, and mixture velocity are introduced. ODEs for these time-dependent expansion parameters are derived by integration along the node. Boiling boundary and its derivative are evaluated by applying the fixed pressure condition at the outlet of riser. Details of the derivations can be found in reference [12].

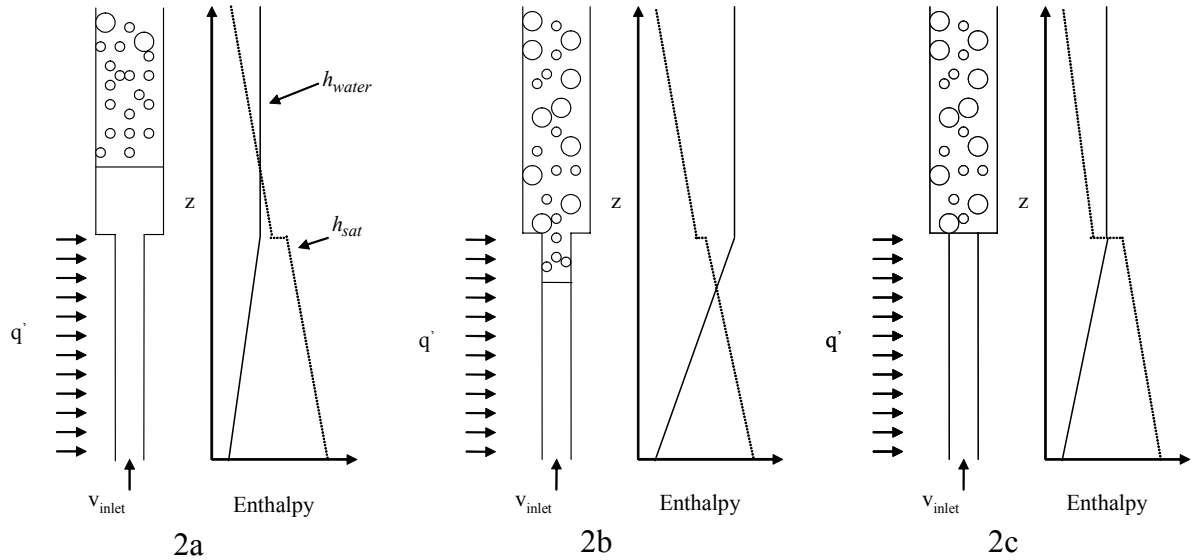

Fig. 2 Profiles of water enthalpy and saturation enthalpy for the three cases: 2a) case 1; 2b) case 2; 2c) case 3.

2.2 Fuel Dynamics and Neutronics Model

The fuel dynamics and neutronics models of Karve et al. [10] are used to couple with the thermal-hydraulic model. These models retain many key elements of the dynamics of BWR systems, such as gap heat conduction between fuel pellet and cladding and different heat convection coefficients for single-phase and two-phase regions, yet are sufficiently simple for large scale parametric analyses. A piece-wise quadratic expansion with time-dependent coefficients is used to represent temperature profiles in the fuel pellet. ODEs for time-dependent coefficients are obtained by application of the variational principle. The neutron and precursor densities are represented by fundamental and first azimuthal modes with time-dependent coefficients. ODEs for the four neutronics variables (n_0, u_0, n_1, and u_1) are derived through the ω-mode approach. Retaining the first azimuthal mode in the model allows the simulation of out-of-phase oscillations. ODEs of thermal-hydraulic model and fuel dynamic and neutronics model are coupled via heat flux (represented by $N_{pch}(t)$, which is a non-dimensional number proportional to the total heat flux inputted into the channel), c_α, the void reactivity feedback coefficient, and c_D, the fuel Doppler reactivity feedback coefficient.

2.3 Poincaré-Andronov-Hopf Bifurcation (PAH-B) Theory and BIFDD

Stability of fixed points of a set of autonomous ODEs, such as those of reduced order model of BWRs, is determined by eigenvalues of the Jacobian at the steady-state. If the real parts of all the eigenvalues are negative, the fixed point is stable, otherwise, unstable. This result is further extended by PAH-bifurcation theory [13], which states that if the right-most eigenvalues are a complex conjugate pair and they cross the imaginary axis with non-zero speed as an operating parameter is changed, there will be periodic solutions (oscillations) in the vicinity of the SB. Frequencies and amplitudes of the periodic solutions are determined by the imaginary parts of the eigenvalues and the distance of the operating point from the SB. In particular, the periodic solutions can be either stable (supercritical PAH-B), or unstable (subcritical PAH-B). From the safety point of view, subcritical PAH-B is more problematic than supercritical PAH-B, since in the former case the unstable periodic solution exists on the stable side of the SB, and given large enough perturbation the system even when operating on the stable side of the SB may evolve into growing amplitude oscillations.

In this study, a stability and bifurcation analysis code BIFDD [14] is utilized to analyze the natural circulation BWR model. Given analytic forms of ODEs and Jacobian, BIFDD evaluates SBs as well as the nature of bifurcation along them.

3. Results

3.1 Effect of Nodalization Schemes

Coupling among thermal-hydraulics, fuel dynamics and neutronics introduces extra feedbacks, which are crucial to the dynamics of the system. However, accurate evaluations of the feedback signals, the void fraction in the channel and fuel temperature rely on nodalization scheme described in section 2.1. The higher the number of nodes in each single-phase or two-phase region, the more accurate is the estimate of the void fraction and fuel temperature. Large number of nodes on the other hand dramatically increase the number of phase variables, leading to computational inefficiency. Therefore, an analysis of the impact of the number of nodes on the results of the stability analysis is carried out first.

Stability boundaries (SBs) are calculated by BIFDD for different nodalization schemes in the so-called subcooling—reactivity parameter space (Figures 3 and 4) for parameter values that roughly correspond to the Dodewaard natural circulation BWR. System pressure of these two calculations are P_{exit} = 7.0 MPa and P_{exit} = 0.4 MPa, respectively. Here, the x axis, ρ_{ext}, is the external reactivity introduced by control rod movement. The y axis, ΔT_{inlet}, is the inlet subcooling (saturation temperature minus inlet temperature). Different nodalization schemes are characterized by *N*, which is the number of nodes in each (single phase and two-phase) region.

Figure 3 shows that at high system pressure, as the number of nodes increases, the SBs converge. Also insufficient nodalization may cause large deviation in both the area of stable regions and in the shapes of SBs from those obtained using sufficiently large number of nodes. Compared to the SB of $N = 16$ case, the one with $N = 1$ significantly over-estimates the area of the stable region. As *N* is increased, the SBs tend to converge. Good convergence of SB is achieved in regions of low and high ρ_{ext} for the $N = 8$ case, but the SB may be over-estimated by as much as 10% in the middle range of ρ_{ext}.

For the low system pressure case (0.4 MPa), Figure 4 shows a much better convergence. Even the SB for the $N = 4$ case is very close to that of the converged SB. SBs for the $N = 8$ and $N = 16$ cases are too close for most values of ρ_{ext} to be distinguished from each other. Results presented in the rest of the paper were obtained using $N = 8$.

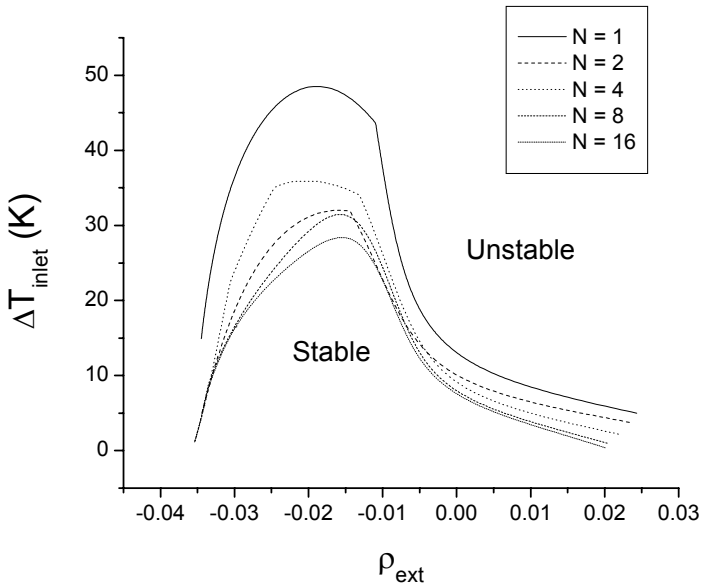

Fig. 3 SBs for different size nodes in $\Delta T_{inlet} - \rho_{ext}$ parameter space for P_{exit} = 7.0 MPa

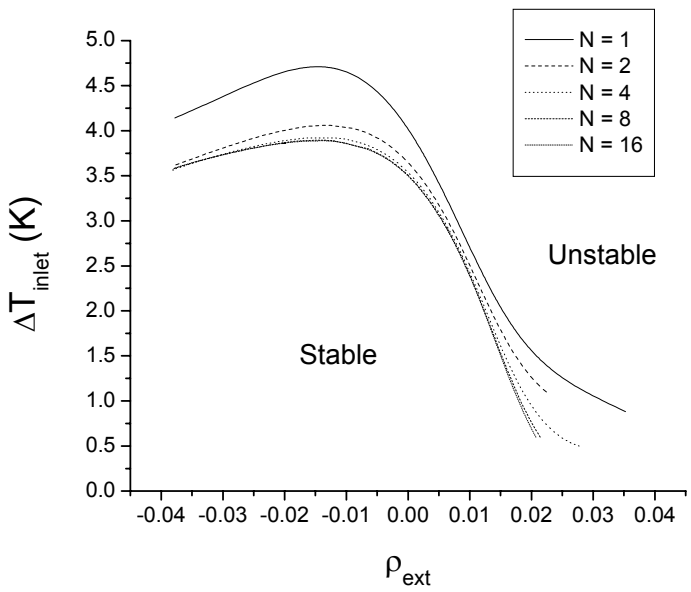

Fig. 4 SBs for different size nodes in $\Delta T_{inlet} - \rho_{ext}$ parameter space for P_{exit} = 0.4 MPa

3.2 In-Phase and Out-Of-Phase Oscillations

A parameter space is divided into stable and unstable regions by a stability boundary. In the unstable region at lease one (complex conjugate pair or real) eigenvalue has positive real part. Figures 5 and 6 show SBs (solid lines) in $\Delta T_{inlet} - \rho_{ext}$ space for system pressure of 7.0 MPa and 0.4 MPa, respectively. Nature of instability that results, as these SBs are crossed, may however vary significantly along different parts of the SB. As shown earlier for forced circulation BWR system, the two rightmost pairs of eigenvalues can be associated with in-phase and out-of-phase oscillations [15]. The relative magnitude of the elements in the corresponding eigenvectors indicate as to which mode—fundamental or first azimuthal—will

become unstable as the corresponding eigenvalue crosses the imaginary axis. It was shown that the eigenvalue pair that corresponds to the first azimuthal mode may cross the imaginary axis before the eigenvalue pair that corresponds to the fundamental mode [15] leading to out-of-phase oscillations. Hence, even for the natural circulation system it is important that boundaries associated with the eigenvalues with the largest and second largest real part be taken into stability consideration. Relative magnitude of the elements in the eigenvector can then be used to identify whether it is the in-phase or the out-of-phase mode that will become unstable as the SB is crossed.

Figures 5 and 6 actually show two boundaries associated with the two pairs of eigenvalues with largest real parts. One of these pairs has zero real part along the boundary with squares, while the second has zero real part along the boundary with triangles. For low system pressure (Figure 6) the two boundaries do not intersect, and hence the entire SB is composed of the boundary associated with one pair of eigenvalue—in this case the one with squares. However, Figure 5, for P_{exit} = 7.0 MPa case, shows that the two boundaries intersect at point X (ρ_{ext} = -0.0335, ΔT_{inlet} = 8.65 K). Hence, the SB (the solid line) is composed of a segment of the boundary with squares and another segment with triangles.

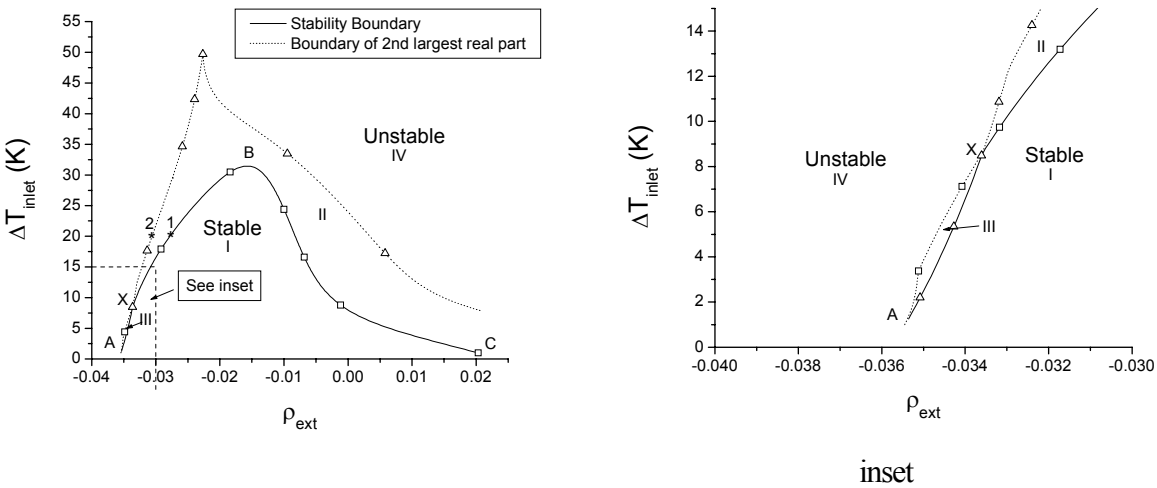

Fig. 5 SB and boundary of the second largest real part when P_{exit} = 7.0 MPa

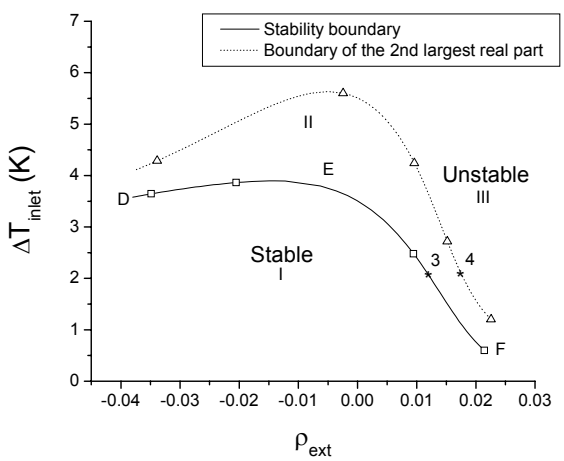

Fig. 6 SB and boundary of the second largest real part when P_{exit} = 0.4 MPa

Characteristic difference of oscillations associated with the two rightmost pairs of complex conjugate eigenvalues is further illustrated by analyzing the eigenvalues and the corresponding eigenvectors at four points on the two boundaries. Point 1 (ρ_{ext} = -0.0278, ΔT_{inlet} = 20.0 K) and point 2 (ρ_{ext} = -0.0306, ΔT_{inlet} = 20.0 K) are on the stability map of system with P_{exit} = 7.0 MPa; point 3 (ρ_{ext} = 0.0124, ΔT_{inlet} = 2.0 K) and point 4 (ρ_{ext} = 0.0179, ΔT_{inlet} = 2.0 K) are on the stability map of system with P_{exit} = 0.4 MPa. Table 1 lists the pure imaginary eigenvalues of the Jacobian E_{imag} and magnitudes of elements corresponding to $n_0(t)$ and $n_1(t)$, EV_{n_0} and EV_{n_1}, in the corresponding eigenvectors at these points. [Here, $n_0(t)$ is the time-dependent coefficient of the fundamental neutron mode, and $n_1(t)$ is the time-dependent coefficient of the first azimuthal mode.] Points 1 and 3 (2 and 4) are chosen to analyze the nature of oscillations associated with the eigenvalues that have a zero real part on the boundary with squares (triangles).

Table 1 E_{imag}, EV_{n_0} and EV_{n_1} at four operating points shown in Figures 5 and 6

	Point 1	Point 2	Point 3	Point 4
E_{imag}	±2.306 *i*	±1.709 *i*	±3.030 *i*	±4.079 *i*
EV_{n_0}	0.156	0.170×10^{-11}	0.00972	0.110×10^{-13}
EV_{n_1}	0.943×10^{-12}	0.0595	0.324×10^{-13}	0.00530

For points 1 and 3, the magnitude of the element of the eigenvector corresponding to $n_0(t)$ is much smaller than that for $n_1(t)$, suggesting large amplitude oscillations in $n_0(t)$, but much smaller amplitude oscillations for $n_1(t)$ at these two points. The pure imaginary eigenvalues at these two points and along the boundary with squares, thus, are called in-phase or fundamental mode eigenvlaues. For points 2 and 4, the magnitude of the element of the eigenvector corresponding to $n_1(t)$ is large, while that of $n_0(t)$ is very small. These eigenvalues, and those corresponding to the boundaries with triangles, are hence called out-of-phase or azimuthal mode eigenvlaues. Therefore, a characteristic change in the nature of oscillation along the SB (solid line) must be expected due to eigenvalue crossing at point X (Figure 5). To the left of point X, segment A-X is the SB due to out-of-phase oscillations. To the right of point X, segment X-B-C is the SB due to in-phase oscillations.

Parameter space in Figure 5 is divided by these boundaries of fundamental and first azimuthal mode eigenvalues into four regions. In region I, both the fundamental and first azimuthal modes are stable. Small perturbation will cause decreasing amplitude oscillations. In region II, the fundamental mode is unstable and the first azimuthal mode is stable. Small perturbations will lead to in-phase oscillations. In region III, the first azimuthal mode is unstable and the fundamental mode is stable. The oscillations are therefore out-of-phase. In the last region (IV), both modes are unstable. Oscillations are therefore a combination of in-phase and out-of-phase modes.

For low system pressure, instead of four regions, three regions of the parameter space are identified. Both modes are stable in region I; fundamental mode is unstable and first azimuthal mode is stable in region II; and both modes are unstable in region III (Figure 6).

3.3 Bifurcation Analyses

In addition to in-phase and out-of-phase, the oscillations in a BWR can also be

characterized by whether they evolve to stable periodic oscillations or to unstable growing amplitude oscillations [13]. As discussed in section 2.3, PAH bifurcation theorem provides us with conditions that lead to one or the other. According to PAH-B theorem, if the periodic solution (oscillations) is in the unstable region, its amplitude is stable and the bifurcation is supercritical; if it is in the stable region, the amplitude is unstable and the bifurcation is subcritical. Nature of PAH-B (supercritical or subcritical) along the SB can be represented by fixed amplitude oscillation curves. Figures 7 and 8 show 7.5% oscillation curves for different segments of the SBs of Figures 5 and 6 in ΔT_{inlet}—($\rho_{ext} - \rho_{ext,critical}$) parameter space. Here $\rho_{ext,critical}$ is the reactivity on the SB. The amplitude of the limit cycle along these curves is about 7.5% of the magnitude of eigenvector elements. In Figure 7a, for the out-of-phase segment A-X, the oscillation curve is in the unstable region, indicating a supercritical PAH-B along the SB. From the out-of-phase segment (A-X) of the SB to in-phase segment X-B, oscillation curve has a jump from the unstable side to the stable side. For ΔT_{inlet} < 28.91 K, the oscillation curve of segment X-B is in the stable region, and type of PAH-B is subcritical. For 28.91 < ΔT_{inlet} < 31.42 K (point B), the oscillation curve returns to the unstable region, and consequently type of PAH-B along this segment of the SB is supercritical. For segment B-C, Figure 7c shows that oscillation curve along the B-C branch is always in the unstable region. Type of PAH-B along this segment is hence supercritical. Similar back-and-forth transitions from sub- to supercritical bifurcations are observed for the low system pressure case. In Figure 8a, the type of bifurcation is supercritical along the D-E branch of the SB. Along the E-F branch of the SB (Figure 8b), when ΔT_{inlet} > 2.762 K, the bifurcation is supercritical; while for ΔT_{inlet} < 2.762 K, it is subcritical.

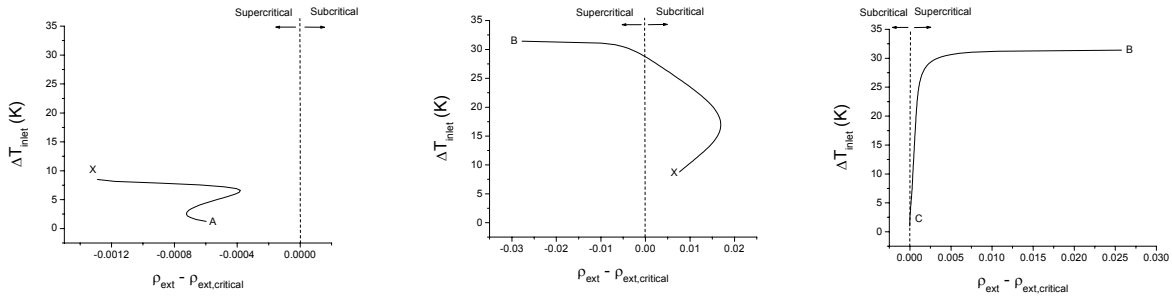

7a 7b 7c

Fig. 7 7.5% oscillation curve along three segments of the SB in Figure 5

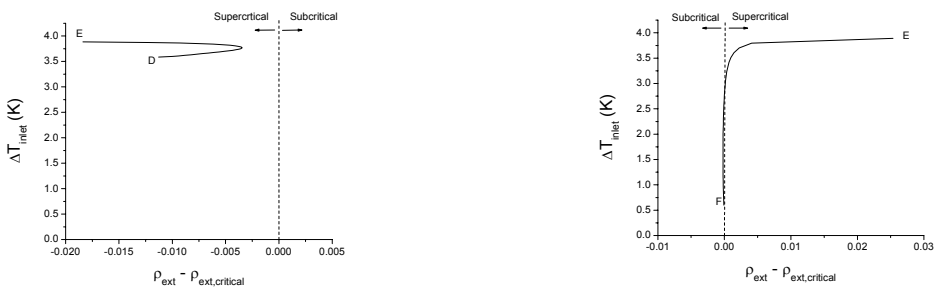

8a 8b

Fig. 8 7.5% oscillation curve along two segments of the SB in Figure 6

For the out-of-phase segment A-X (Figure 7a) and low ΔT_{inlet} region of the in-phase

segment B-C (Figure 7c), deviations of ρ_{ext} from its critical value required for the 7.5% amplitude, are much smaller than those for the segment X-B and high ΔT_{inlet} region of the segment B-C, indicating that much larger amplitude oscillations (in-phase or out-of-phase) may result for the same deviation along the SB in the low subcooling region than those along the SB in the high subcooling region. Large amplitude oscillations at lower inlet subcooling are due to longer two-phase regions in the channel and riser. Similar trend can be found in the low system pressure case (Figure 8).

The change in characteristic of bifurcation (supercritical or subcritical) and change characteristic of oscillations (in-phase or out-of-phase) along the SB, thus, reveal complexity of the dynamic behavior of the coupled natural circulation BWR system.

3.4 Sensitivity Analysis for Low System Pressure Case

Effect of operating parameters other than ΔT_{inlet} and ρ_{ext} on the SBs is investigated. Since behavior of two-phase natural circulation systems under high system pressure conditions (close to 7.0 MPa) is relatively better understood, we focus on sensitivity of operating parameters when the system pressure is relatively low. To study effect of system pressure, we plot SBs in ΔT_{inlet} — ρ_{ext} parameter space for five different values of P_{exit} (Figure 9a). Impact of a change in P_{exit} on systems with relatively large pressure (P_{exit} = 1.5, 1.0 MPa) is different from that on systems at low pressure (P_{exit} = 0.4, 0.3, 0.2 MPa). Stable region decreases as P_{exit} decreases if the system pressure is relatively high, especially for small

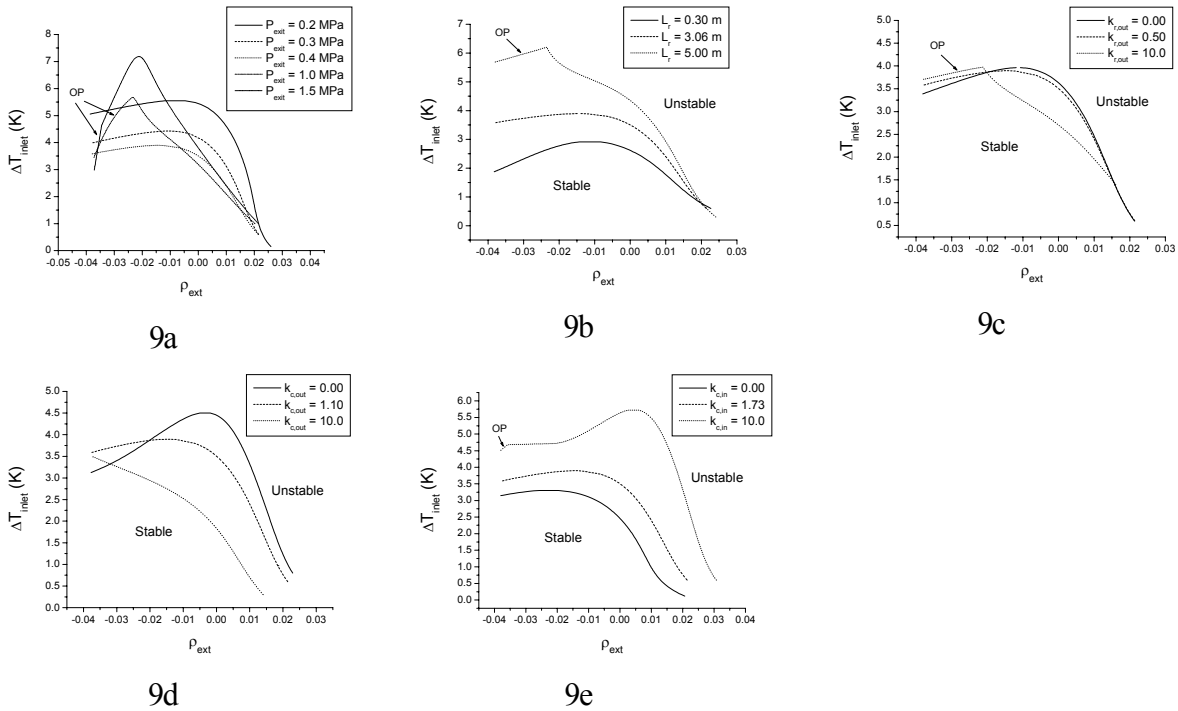

Fig. 9 Sensitivity analysis results for different operating parameters. Out-of-phase oscillation SBs are indicated by OP. A change in slope of the SB indicates transition to in-phase SB.

values of ρ_{ext}. Thus, a drop in P_{exit} has a destabilizing effect under these conditions. If the system pressure is relatively low, however, a drop in P_{exit} causes the stable region to increase. Therefore, instead of destabilizing, it has a stabilizing effect on the dynamics of the system. Comparing these results with those of pure thermal-hydraulics model [12], where a drop in system pressure is a destabilizing factor, this

new stabilizing effect can be attributed to the coupling between system thermal-hydraulics and neutron kinetics. At low system pressure, without neutronics coupling, small perturbation can quickly grow due to two-phase flow instability. In the coupled system, however, void fraction feedback acts as a stabilizing force. Perturbations in void fraction lead to negative feedback of reactivity, which suppresses thermal-hydraulic perturbations.

Figure 9b shows the effect of riser length L_r, for P_{exit} = 0.4 MPa case. In natural circulation system, increasing L_r increases the driving force leading to higher flow rate. Therefore, it has a strong stabilizing effect. However, Figure 9b also shows that out-of-phase oscillations are possible at low reactivity for long risers. Effect of pressure loss coefficient at riser outlet $k_{r,out}$ is not as strong as those for P_{exit} and L_r (Figure 9c), but SBs indicate the possibility of out-of-phase oscillations for low reactivity if $k_{r,out}$ is high. Figure 9d shows the effect of an increase in pressure loss at the outlet of the core. Increasing $k_{c,out}$ generally tends to cause a loss of stability. The last operating parameter studied is the pressure loss coefficient at the core inlet, $k_{c,in}$. As shown in Figure 9e, increasing of $k_{c,in}$ has a strong stabilizing effect.

3.5 Numerical Simulations

Numerical simulations are carried out to gain further insight into the dynamics of the coupled system as well as to examine the results obtained using BIFDD. Eight points on the stability maps of high and low pressure systems are chosen for numerical simulations. These points are shown in Figures 10a and 10b. Table 2 lists operating parameters as well as characteristics of bifurcation and nature of oscillations (in-phase or out-of-phase) predicted by BIFDD.

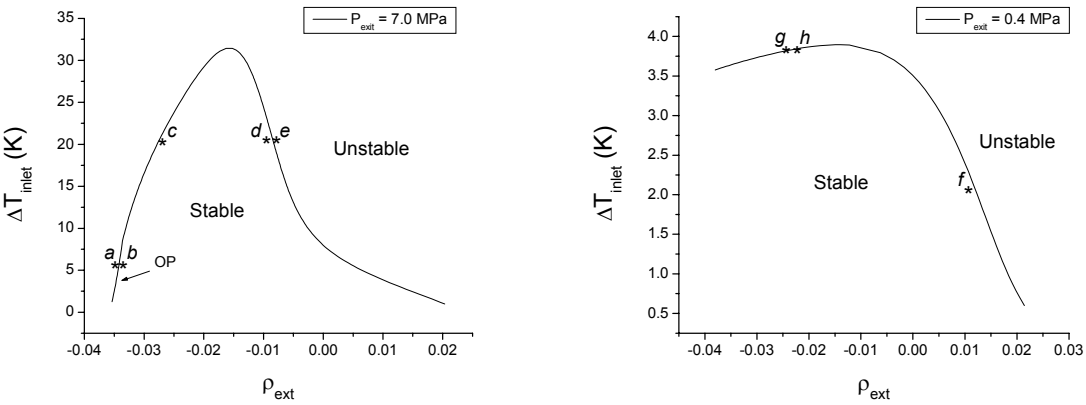

10a 10b

Fig. 10 Operating points for numerical simulations in the SBs, 10a) P_{exit} = 7.0 MPa; 10b) P_{exit} = 0.4 MPa

Points *a* and *b* are close to out-of-phase segment of the SB (Figure 10a). Point *a* is in the unstable region, while point *b* is in stable region. Bifurcation along this segment of the SB is supercritical. Figure 11 shows results of numerical simulation for parameter values corresponding to point *a*. As expected, stable amplitude limit cycle of $n_1(t)$ and very small amplitude of $n_0(t)$ result. Figure 12 (for point *b*) shows decreasing amplitude oscillations for both $n_0(t)$ and $n_1(t)$. Points *c*, *d* and *e* are close to in-phase segment of the SB. Bifurcation at point *c* is subcritical; while those for points *d* and *e* are supercritical. Figure 13, corresponding to point *c*, shows increasing amplitude of $n_0(t)$ (and decaying $n_1(t)$) for large perturbation even though point *c* is in the stable region, consistent with the subcritical nature of the bifurcation. For point *d* (in stable region) and *e* (in unstable region), perturbations lead to decreasing

amplitude oscillations (point *d*) and stable limit cycle oscillations (point *e*) for $n_0(t)$ while decreasing amplitude oscillations result for $n_1(t)$ in both cases (Figures 14 and 15).

Table 2 Operating points for numerical simulations

	P_{exit} (MPa)	ρ_{ext}	ΔT_{inlet} (K)	Characteristics of oscillations	Characteristics of PAH-B
Point *a*	7.0	-0.03413	6.0	Out-of-phase	Supercritical
Point *b*	7.0	-0.03400	6.0	Out-of-phase	Supercritical
Point *c*	7.0	-0.02781	20.0	In-phase	Subcritical
Point *d*	7.0	-0.00840	20.0	In-phase	Supercritical
Point *e*	7.0	-0.00823	20.0	In-phase	Supercritical
Point *f*	0.4	0.01237	2.0	In-phase	Subcritical
Point *g*	0.4	-0.02570	3.8	In-phase	Supercritical
Point *h*	0.4	-0.02540	3.8	In-phase	Supercritical

For the case of low system pressure, Figures 16, 17, and 18 show that oscillations at points *f*, *g*, and *h* are in-phase as suggested by the stability analysis. Large perturbation at point *f*, which is in the stable region, causes increasing amplitude oscillation consistent with the subcritical bifurcation there. Perturbations at point *g* (unstable region), and *h* (stable region) cause limit cycle and decreasing amplitude oscillations, respectively, for $n_0(t)$. Numerical simulations of system with high and low system pressures agree with predictions of BIFDD satisfactorily.

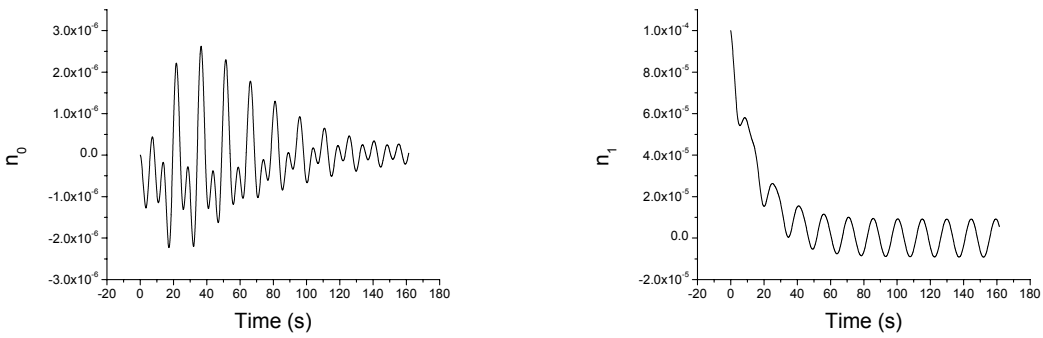

11a 11b

Fig. 11 Time evolutions of $n_0(t)$ and $n_1(t)$ at point *a* in Figure 10a

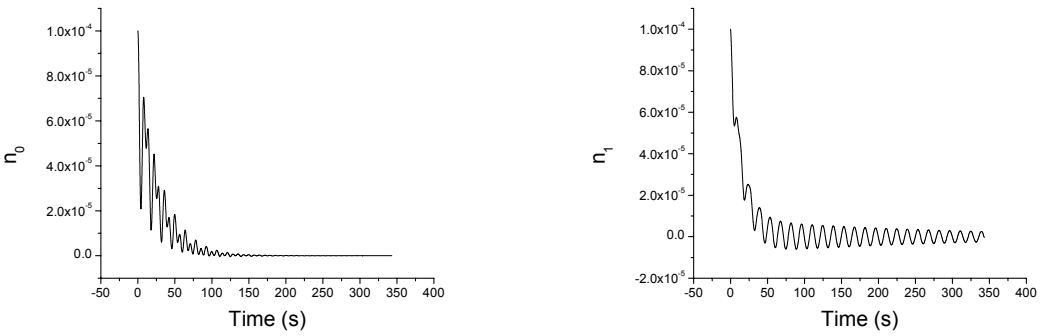

12a 12b

Fig. 12 Time evolutions of $n_0(t)$ and $n_1(t)$ at point *b* in Figure 10a

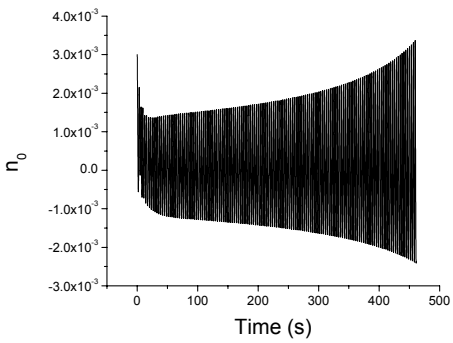

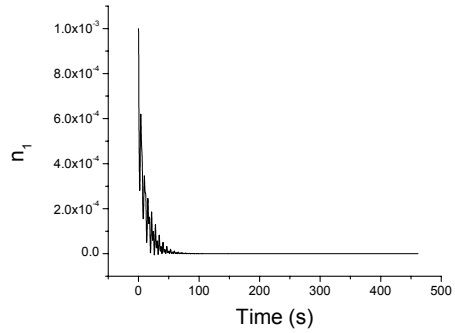

13a 13b

Fig. 13 Time evolutions of $n_0(t)$ and $n_1(t)$ at point *c* in Figure 10a after large amplitude perturbation. System is stable for small amplitude perturbations

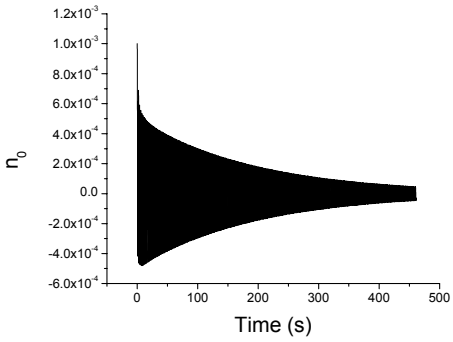

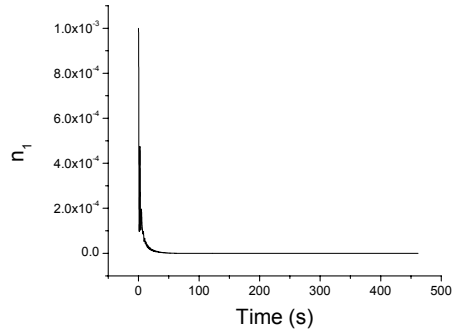

14a 14b

Fig. 14 Time evolutions of $n_0(t)$ and $n_1(t)$ at point *d* in Figure 10a

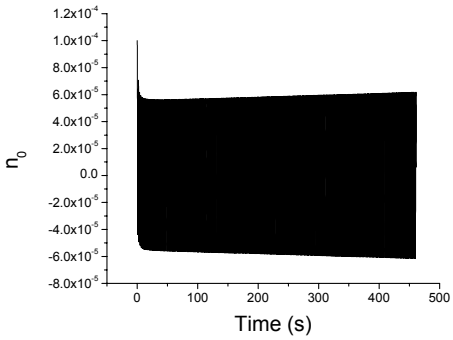

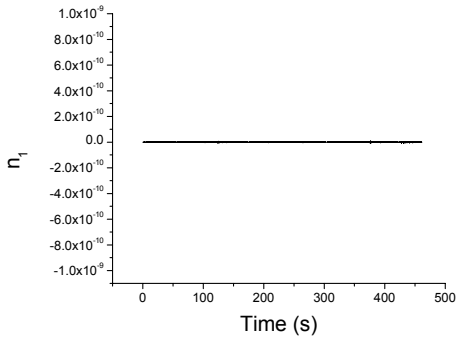

15a 15b

Fig. 15 Time evolutions of $n_0(t)$ and $n_1(t)$ at point *e* in Figure 10a

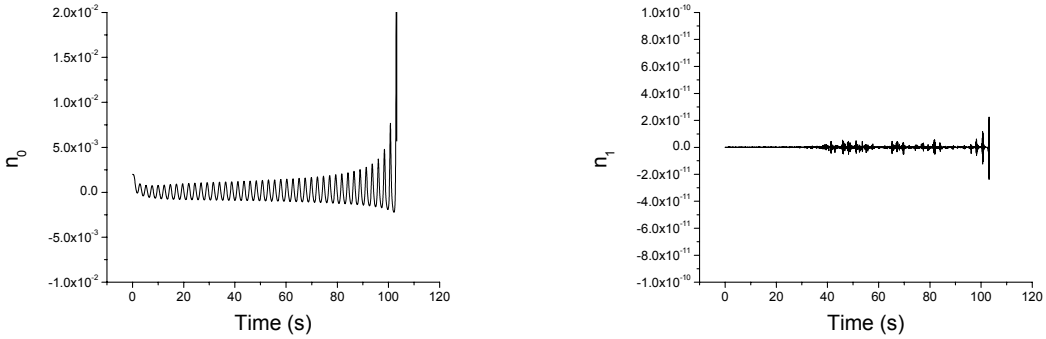

16a 16b

Fig. 16 Time evolutions of $n_0(t)$ and $n_1(t)$ at point *f* in Figure 10b after large amplitude perturbation. System is stable under small amplitude perturbations

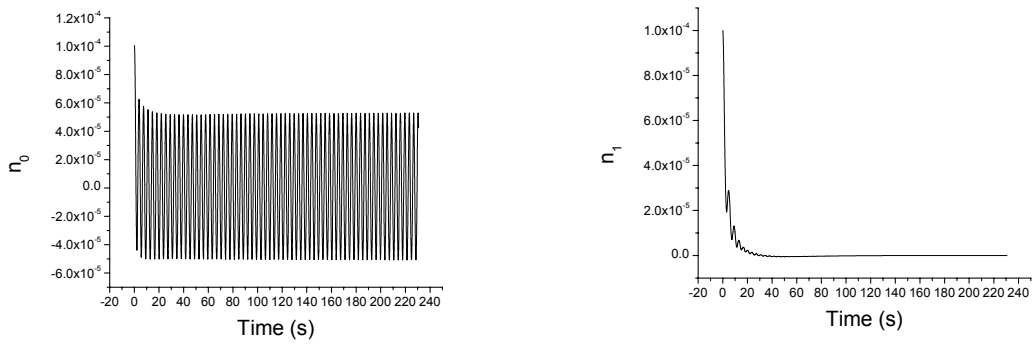

17a 17b

Fig. 17 Time evolutions of $n_0(t)$ and $n_1(t)$ at point *g* in Figure 10b

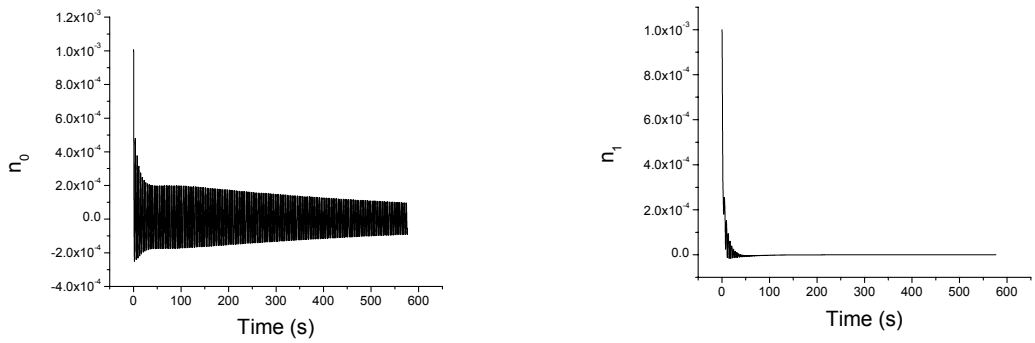

18a 18b

Fig. 18 Time evolutions of $n_0(t)$ and $n_1(t)$ at point *h* in Figure 10b

4. Summary

A new natural-circulation BWR model that allows local pressure dependence of water saturation enthalpy and includes fundamental and first azimuthal modes for neutronics is presented. ODEs of this model are derived through weighted residual and variational principle approaches. A node-size sensitivity analysis shows that proper nodalization is important to accurately capture the SB. Both in-phase and out-of-phase oscillations as well as supercritical and subcritical bifurcations can occur along the SBs for

both high and low system pressures. Sensitivity analysis of various operating parameters is also carried out. It is shown that increasing system pressure may lead to a more stable or a less stable system depending upon the value of the absolute system pressure. Increasing pressure loss coefficient at the outlet of core or riser has a destabilizing effect, while increase of pressure loss coefficient at the core inlet has a stabilizing effect. Numerical simulation results confirm findings of stability and bifurcation analyses.

References

1) R. Challberg, Y. Cheung, S. Khorana, H. Upton, "ESBWR evolution of passive features," Proceedings of the Sixth International Conference On Nuclear Engineering (ICONE-6), ASME, San Diego, USA, May 10-15 (1998)
2) J. March-leuba, J. Rey, "Coupled thermal hydraulic neutronic instabilities in boiling water nuclear reactors: A review of the state of the art," Report at OECD committee of specialist meeting on safety of nuclear instabilities, Karlsruhe, Germany, April 1-3 (1992)
3) J. March-Leuba, E. Blakeman, "A mechanism for out-of-phase power instabilities in boiling water reators," Nucl. Sci. Eng., **107**, 173 (1991)
4) S. Jiang, D. Emerdorfer, "Subcooled boiling and void flashing in a natural circulation system at heating reactor conditions," Kernitechnik, **58**, 273 (1993)
5) J. Chiang, M. Aritomi, R. Inoue, M. Mori, "Thermo-hydraulics during start-up in natural circulation boiling water reactors," Nucl. Eng. Des., **146**, 241 (1994)
6) T. van der Hagen, A. Stekelenburg, D. van Bragt, "Reactor experiments on type-I and type-II BWR stability, " Nucl. Eng Des., **200**, 177 (2000)
7) A. Manera, T. van der Hagen, "Stability of natural-circulation-cooled Boiling Water Reactors during startup: experimental results, " Nucl. Tech., **143**, 77 (2003)
8) F. Inada, T. Ohkawa, "Thermo-hydraulic instability of natural circulation BWRs (Explanation on instability mechanisms at start-up by homogeneous and thermo-dynamics equilibrium model considering flashing effect)," Proc. of International Conference on New Trends in Nuclear System Thermohydraulics, Pisa Italy, May 30~Jun 2, (1994)
9) D. van Bragt, "Analytical modeling of boiling water reactor dynamics," Ph.D Thesis, Delft University Press(1998)
10) A. Karve, Rizwan-uddin, J. Dorning, "Out of phase power oscillations in boiling water reactors," Proc. Of the Joint Int. Conf. On Mathematical Methods and Super-computing, Saratoga Springs, NY, Oct. 5-9, 1997, **2**, 1633 (1997)
11) Q. Zhou, Rizwan-uddin, "Stability and bifurcation analyses of boiling natural circulation loop under low pressure, " ANS Transactions, New Orleans, Louisiana, November 16-20, (2003)
12) Q. Zhou, "Stability and bifurcation analyses of reduced-order model of forced- and natural circulation BWRs, " Ph.D. Thesis, University of Illinois at Urbana-Champaign, in preparation
13) B. Hassard, N. Kazarinoff, Y. Wan, "Theory and applications of Hopf bifurcation," Cambridge University Press, New York (1981)
14) B. Hassard, "A code for bifurcation analysis of autonomous delay-differential systems," Proc. Oscillation, Bifurcation and Chaos, Canadian Mathematical Society, 447 (1987)
15) Q. Zhou, Rizwan-uddin, "Bifurcation analyses of in-phase and out-of-phase oscillations in BWRs," Proceedings of PHYSOR 2002, Seoul, Korea, October 7-10, (2002)